한국해양환경·에너지학회지
J. Korean Soc. Mar. Environ. Energy
Vol. 20, No. 3, 136-144, August 2017

https://doi.org/10.7846/JKOSMEE.2017.20.3.136
ISSN 2288-0089(Print) / ISSN 2288-081X(Online)

Original Article

다단식 월파형 파력발전장치의 구조물 형상이 추출효율에 미치는 영향 연구

시리랏 중룽루엥타원 · 현범수†
한국해양대학교 조선해양시스템공학부

Effects of Structure Geometry on Energy Harvesting Efficiency of Multi-Stage Overtopping Wave Energy Converters

Sirirat Jungrungruengtaworn and Beom Soo Hyun†
Division of Naval Architecture and Ocean Systems Engineering, Korea Maritime and Ocean University, Busan 49112, Korea

요 약

다단식 월파형 파력발전장치의 구조물 형상이 성능에 미치는 영향을 연구하기 위하여 RANS방정식을 이용한 2차원 전산해석을 실시하였다. 램프의 치수가 가변적인 두 개의 대표적인 구조물 형상에 대하여 전 수력학적 효율 관점에서 성능을 비교하였다. 수치해석 결과 가변 램프의 치수가 효율에 미치는 영향은 그리 크지 않았으나, 고정식 방파제에 이를 적용한 결과 다단식 램프의 잠긴깊이가 변함에 따라 월파성능에 다양한 영향을 미침을 알 수 있었다. 방파제형 다단식 장치가 단일 램프 및 다단식 월파장치만 설치된 경우와 비교하여 확연한 성능 증가가 얻어졌으며, 잠긴깊이가 증가할수록 방파제의 성능이 향상되는 경향도 확인되었다.

Abstract – The effects of structure geometry of multi-stage overtopping wave energy converter (OWEC) are investigated using two-dimensional RANS (Reynolds-averaged Navier-Stokes)-based numerical simulation. The performance based on overall hydraulic efficiency of two design layouts: overlap ramp of non-adaptive and adaptive devices are compared. The numerical results show that the overall hydraulic efficiency of both layouts are approximately on par. In addition, the effect of submerged depth of multi-stage device installed on breakwater has been studied. This land-based type gives convergence trend of efficiency. For small value of submerged depth, the performance is increasing for increasing the variable. Further increasing the depth, the performance tends to converge to a certain value.

Keywords: Wave Energy Converter(파력발전장치), Overtopping(월파형), Multi-Stage(다단식), Overlap Ramp(오버랩 램프), Breakwater(방파제)

1. Introduction

The available energy resources in the world can be categorized into two kinds: Non-renewable energy, i.e., oil or fossil fuels, and Renewable energy, i.e., solar, wind or wave energy. Over the past decades, renewable energy becomes one of the most interesting research topics. Marine renewable energy is huge and available in the forms of tidal, current, offshore wind, ocean thermal, and sea wave.

Extracting energy from wave has advantage over other kinds of renewable energy because sea waves offer the greatest energy density compared to other renewable energy sources (Clément et al.[2002]). Moreover, harvesting wave energy has little environmental impact. It has been estimated that the potential worldwide wave energy is approximately 2 TW (Thorpe[1999]). In 2014, it is reported that there is 3730 kW installed capacity of wave energy utilization in UK, 700 kW in Portugal, 296 kW in Spain, 180 kW in Sweden, 200 kW in Norway, 350 kW in China, 500 kW in Korea, 16 kW in Singapore (Brito and Vilate[2014]).

†Corresponding author: bshyun@kmou.ac.kr

Generally, a wave energy converter (WEC) consists of two systems or devices: wave capture device and power take-off system (PTO). The former directly interacts with incident wave and subsequently extracts energy from it. The latter simultaneously take-off energy from wave capture device and accumulate in an energy storage, i.e., battery or hydraulic accumulator.

There are many concepts of wave energy converter introduced worldwide. They can be categorized by operation mode, for example, oscillating buoy, oscillating water column, and overtopping device. The performance of overtopping wave energy converter (OWEC) has been investigated by the means of experiments and numerical simulations. Scientists and researchers have focused on the influence of geometry on the discharge, volume flow rate into the reservoir, which directly determines the performance of an OWEC and consequently the generation rate of useful electrical energy.

The effects of geometry of single-stage device, such as ramp angle, ramp shape and hydro head of the ramp on the overtopping discharge, have been studied by many researchers (Liu *et al*.[2008, 2009a,b]; Nam *et al*.[2008]; Victor *et al*.[2011]). Moreover, the application of multi-stage device has been suggested and studied in order to increase the performance of OWEC. An example of multi-stage device is the Seawave Slot-cone Generator (SSG) overtopping wave energy converter which is shown in Fig. 2.

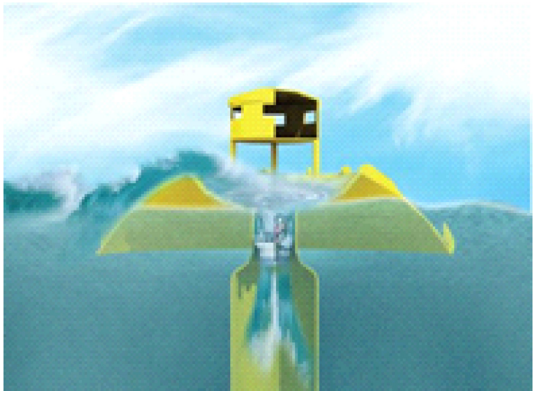

Fig. 1. Spiral-reef overtopping device (single-stage OWEC type) (Nam *et al*.[2008]).

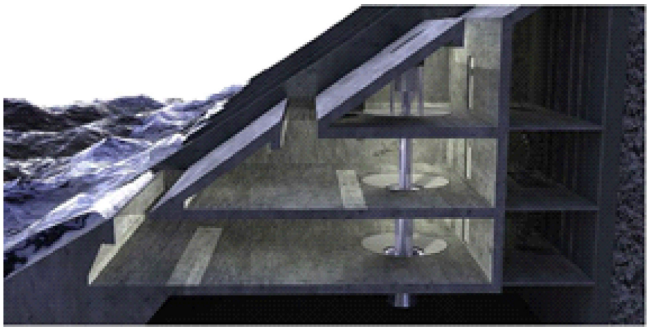

Fig. 2. Section of a three-levels SSG overtopping device (multi-stage OWEC type) (Margheritini *et al*.[2009]).

In general, the wave energy harvested by multi-stage device is effective in variable and wide range of wave condition. Many studies (Kofoed[2005]; Vicinanza and Frigaard[2008]; Margheritini et al.[2009]; Tanaka et al.[2015]) expect to find an optimal design to gain performance enhancement. Jungrungruengtaworn and Hyun[2017] studied the effect of slot width as well as adaptive slot width of multi-stage device on the overall hydraulic efficiency and concluded that the optimal hydraulic efficiency is obtained at an intermediate value of the studied parameters depending on design layouts. Generally, the overall hydraulic efficiency of wave energy converters, based on the overtopping principle, can be 20-35% when a single reservoir is used, and up to 45-50% for structure with reservoirs at 4 levels (Kofoed[2002]). In addition, several researchers (Kofoed[2006]; Minami and Tanaka[2015]; Van der Meer and Janssen[1995]), proposed equations used to predict the overtopping flow rate of single- and multi-stage devices which are useful to validate numerical results.

Due to the complicated geometry of the multi-stage device, there are many other variables, affecting the energy harvesting efficiency of the device, that have not been studied yet. In the present study, two sets of multi-stage OWEC with different geometric design are numerically investigated: (1) devices with different overlap ramp and (2) devices with different submerged depth. The goals of this study are to find a geometry giving optimal efficiency and to gain a better understanding of unsteady water flow mechanisms.

2. Numerical simulations

Two-dimensional numerical simulation of multi-stage OWEC devices are investigated by using a commercial CFD solver ANSYS FLUENT V.17. The finite volume method is applied to the continuity and the Reynolds Averaged Navier-Stokes (RANS) equations for viscous, incompressible, two-dimensional flow. In order to track and locate the free surface, two-phase volume of fluid (VOF) method is utilized. The standard k-ε turbulence model is applied for turbulence closure.

2.1 Numerical domain

The numerical wave tank domain used in the present study is shown in Fig. 3. The domain is 300 m long and has water depth of 20 m approximately corresponding to 5.4 λ and 0.36 λ respectively, where λ is the wavelength calculated by dispersion rela-

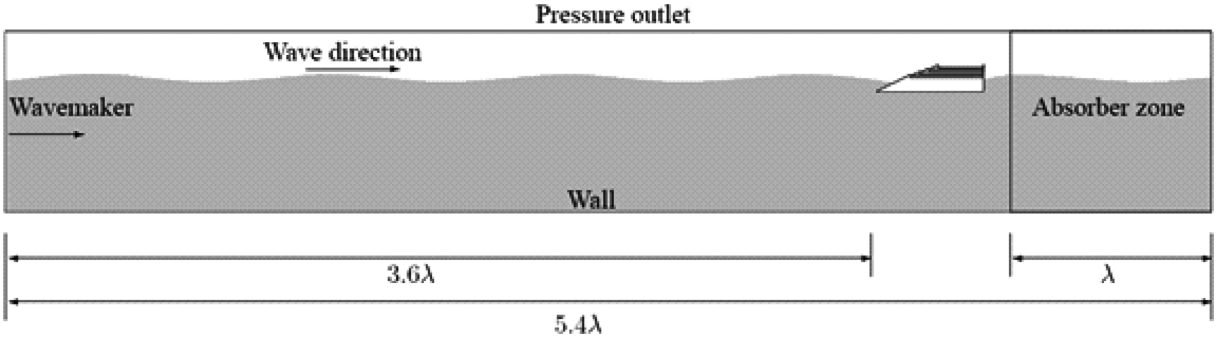

Fig. 3. Two-dimensional numerical wave tank used to simulate wave flow behavior.

tion. This condition falls in the intermediate water depth. The length of absorber zone equals to a wavelength (1 λ). If this zone is too short, the wave energy could not be effectively absorbed. On the contrary, if this zone is too long, it affects the computational expense. Moreover, numerical wave probes are employed in front of and behind the device in order to record surface elevation. The conditions are applied differently to boundaries surrounding the domain. Wall condition combined with dynamics mesh model is applied on the left boundary to generate wave. The function of wave generation is described by a UDF (User-defined function) code in this paper is based on the previous study (Jungrungruengtaworn and Hyun [2017]). The motion of the piston type wavemaker $x(t)$ is defined by:

$$x(t) = \frac{x_0}{2}\left(1 - e^{\frac{-5t}{2T}}\right)\sin\omega t \tag{1}$$

where x_0 is the maximum displacement of the wavemaker and ω is the angular frequency.

The pressure outlet and open channel flow condition combined with porous media model is used at outlet (right boundary) acting as a wave absorber which is similar to the boundary conditions of numerical wave tank used by Du and Leung[2011] and Hu and Liu[2014]. The porous media condition is defined by an additional momentum source term which is added to the Navier-Stokes equations as:

$$\rho\left(\frac{\partial v}{\partial t} + v\cdot\nabla v\right) = (-\nabla p + \mu\nabla^2 v + f) + S_i \tag{2}$$

and

$$S_i = -\left(\frac{\mu}{\alpha}v_i + C_2\frac{1}{2}\rho|v_i|v_i\right) \tag{3}$$

where S_i is the additional source term, consisting of two parts: a viscous loss term and an inertial loss term, for the i-th (x, y or z) momentum equation, $|v_i|$ is the velocity magnitude, $1/\alpha$ is the viscous resistance coefficient, and C_2 is the inertial resistance factor.

The viscous resistance coefficient ($1/\alpha$) is the key parameter in order to define the rate of absorption which has been investigated and shown the accuracy of the wave profile in the previous study (Jungrungruengtaworn and Hyun[2017]). Pressure outlet and wall condition are applied on top and bottom boundary respectively.

In the present study, adaptive refinement is utilized in order to construct grid system of the computational domain. A dense or more refined mesh is generated in regions of interest: the vicinity of free surface and OWEC device. The mesh size is dependent on the wave height and length. In this work, the number of cells per wave height is 20 cells and 100 cells per wavelength is used following the previous study (Jungrungruengtaworn and Hyun [2017]) which is considerably dense compared to the grid system suggested by Connell and Cashman[2016].

2.2 Optimum design

The optimization of the OWEC design concerns particularly the ramp geometry in order to maximize the energy captured by the reservoirs. There are two strategies to achieve the goal: devices with different overlap ramp and devices with different submerged ramp.

The former investigation focuses on the influence of overlap ramp on the hydraulic performance. The base-line model is based on non-adaptive device which is schematically illustrated in Fig. 4b. The ramp height consists of two parts, the submerged depth R_s and freeboard height R_{c4} that both parameters are fixed as 2 m. The slope of each ramp S is defined as the ratio between the ramp height R and horizontal ramp length L which is kept constant as S=1/2 for both freeboard and draught parts. This consequently results in the $3\overline{w}$ extended length of the ramp.

These multi-stage devices have three extra slots which are defined as w_1 (the lowest), w_2 (the middle) and w_3 (the highest). The adaptive layout gives difference in size of the slots as

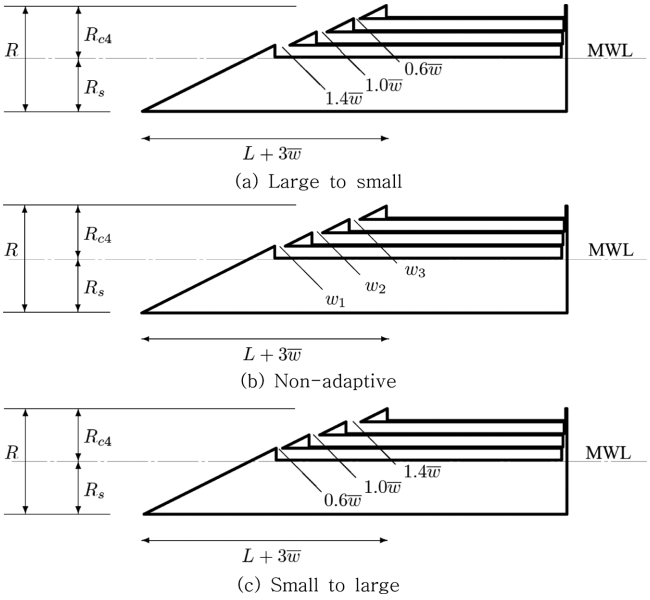

Fig. 4. Layouts of non-overlap ramp multi-stage devices base on the relative slot width of 0.2.

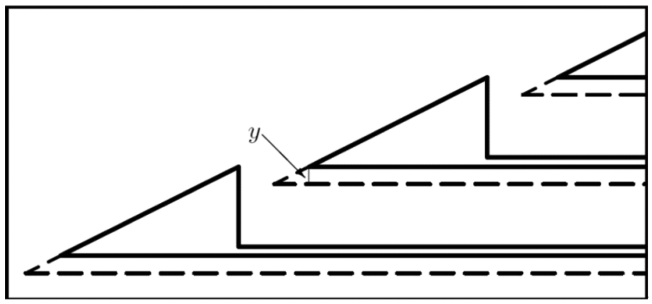

Fig. 5. Example of overlap ramp layout of non-adaptive device.

$\Delta w=w_2-w_1=w_3-w_2$, so that the average width of each device is $\overline{w}=w_2$ which is fixed as 0.4 m in the present study. Moreover, the parameter slot width, $\overline{w}$ is represented in dimensionless form namely relative slot width as: $\overline{w}/R_{c4}$ of 0.2. The adaptive device has two layouts: reservoir width varies from large to small ($w_1=1.4\overline{w}$) and vice versa. The illustration of overlap distance is shown in Fig. 5 and is defined by parameter y that is varied within the range of 0.025 to 0.100 m with a 0.025 m increment. This design is applied to both adaptive and non-adaptive devices.

Table 1. Slot width of multi-stage devices

Device	$w_i/\overline{w}$		
	Slot 1	Slot 2	Slot 3
Large to small	1.4	1.0	0.6
Non-adaptive	1.0	1.0	1.0
Small to large	0.6	1.0	1.4

The slot width of non-adaptive and adaptive devices are summarized in Table 1. The distance of slot width is measured horizontally at crest level. Fig. 4 shows the layouts of non-overlap ramp multi-stage devices based on the relative slot width of 0.2 which is corresponding to the Table 1.

The second investigation concerns the influence of submerged ramp on the performance of land-based OWEC. The parameter R_s is varied within the range 2 to 8 m with a 2 m increment. The schematic illustration of OWEC device installed on breakwater is shown in Fig. 6.

2.3 OWEC performance

The overall efficiency of OWEC device consists of four partial efficiencies, i.e., hydraulic efficiency, reservoir efficiency, turbines efficiency and generator efficiency. In the present study, the numerical results are represented by the hydraulic efficiency η calculated based on crest levels $R_{c,i}$ and averaged discharge Q_i. The hydraulic efficiency η is defined as the ratio between the potential power P_{crest} in the overtopping water and the power in the incident wave P_{wave} which is also used by Margheritini *et al.*[2009] and Tanaka *et al.*[2015] as:

$$\eta = \frac{P_{crest}}{P_{wave}} \tag{4}$$

where

$$P_{crest} = \sum_{i=1}^{n} Q_i \rho g R_{c,i} \tag{5}$$

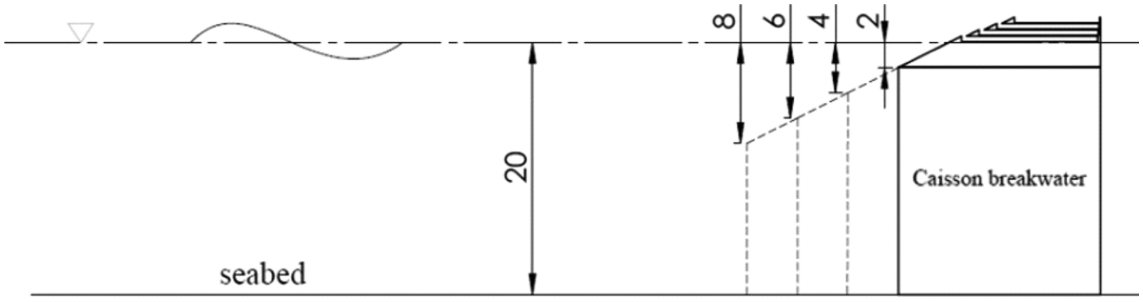

Fig. 6. Schematic of multi-stage device to study the effect of submerged depth on performance.

and

$$P_{wave} = \frac{1}{8}\rho g H^2 c \frac{1}{2}\left[1+\frac{2kd}{\sinh(2kd)}\right] = Ecn \quad (6)$$

here ρ is the water density, g is the gravitational acceleration, Q_i is the average overtopping flow rate per unit length of the i^{th} reservoir, $R_{c,i}$ is the crest height of the i^{th} reservoir and H is the wave height.

The wave energy flux or wave power shown in the Eq. 6 consists of three terms: wave energy density E, phase velocity c and factor n. The factor n is relates to the region of water depth, for deep water, n=1/2 and for shallow water, n=1.

The incident, reflected and transmitted wave power can be calculated using Eq. 6, when the height or amplitude of these waves is known. The transportation of energy conservation of the overtopping phenomenon can be explained by:

$$P_{wave} = P_{crest} + P_r + P_t + P_L \quad (7)$$

here P_r is the reflected wave power, P_t is the transmitted wave power and P_L is the dissipated wave power or loss.

Since the wave power is proportional to H^2 or a^2 then the dimensionless wave energy in reflection wave is proportional to K_r^2 where K_r is the reflection coefficient which is ratio between the reflected and incident wave amplitudes: K_r=a_r/a_i. In addition, Eq. 7 can be expressed in dimensionless form by:

$$1 = \eta + K_r^2 + K_t^2 + L \quad (8)$$

where K_r^2 is the reflection rate, K_t^2 is the transmission rate and L is the loss rate which is defined as ratio between the dissipated wave power P_L to the incident wave power: L=P_L/P_{wave}. This equation is similar to transportation of energy conservation used by Tanaka *et al*.[2015].

The reflection coefficient used in Eq. 8 can be determined using recorded wave profiles, since the free surface elevation is assumed to be the superposition of sinusoidal incident and reflected wave trains. A detailed explanation of the method is summarized by Isaacson [1991]. By using two fixed numerical wave probes, the incident and reflected wave amplitudes can be represented respectively by:

$$a_i = \frac{1}{2|\sin\Delta|}\sqrt{A_1^2 + A_2^2 - 2A_1A_2\cos(\Delta+\delta)} \quad (9)$$

and

$$a_r = \frac{1}{2|\sin\Delta|}\sqrt{A_1^2 + A_2^2 - 2A_1A_2\cos(\Delta-\delta)} \quad (10)$$

where A_n is the measured amplitude of the n^{th} probe, Δ is the dimensionless distance between two probes, and δ is the measured phase angle of second probe relative to that of the first probe and is obtained by fast Fourier transform (FFT) algorithm. Similarly, the transmission coefficient is expressed as the ratio between the transmitted and incident wave amplitudes: K_t=a_t/a_i which can be calculated using measured wave profiles.

3. Results and discussion

The characteristics of ocean wave used in this study are shown in the Table 2 in which the generated incident wave height H of 2 m and the wave period T of 6 s is utilized following Liu *et al*.[2008]. This is corresponding to wavelength λ of 55.56 m.

3.1 Combination of overlap ramp and adaptive slot width

The overlap distance y, which is presented in dimensionless form as $y/\overline{w}$, is shown in the Table 3. This overlap design, i.e.,

Table 2. Ocean wave conditions

Wave height, H [m]	2.0
Wave period, T [s]	6.0
Water depth, d [m]	20.0
Wave steepness, H/λ [-]	0.036
Relative wave height, H/d [-]	0.1

Table 3. Parameters condition studying effect of overlap ramp

Submerged depth, R_s [m]	2.0
Relative freeboard, R_{c4}/H [-]	1.0
Relative slot width, $\overline{w}/R_{c4}$ [-]	0.2
Overlap distance, y [m]	0.025, 0.05, 0.075, 0.10
Relative extended ramp, $y/\overline{w}$ [-]	0.0625, 0.125, 0.1875, 0.25

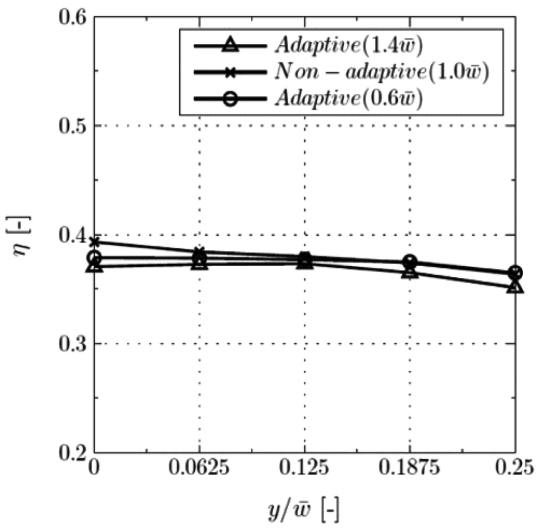

Fig. 7. Effect of overlap ramp applied to multi-stage devices on overall hydraulic efficiency as function of relative extended ramp. The non-overlap ramp is represented by the relative extended ramp $y/\overline{w}$=0.

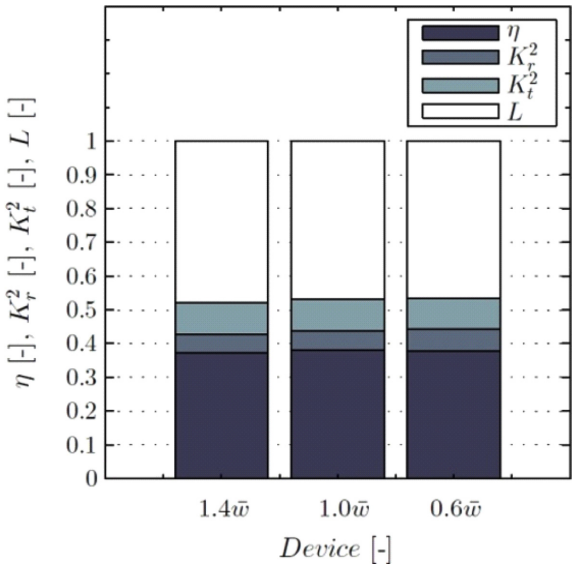

Fig. 8. Comparison of overall hydraulic efficiency, reflection, transmission and loss rates of overlap ramp non-adaptive and adaptive device base on $y/\overline{w}$=0.125.

extended the ramp of each extra slot, is applied to both adaptive and non-adaptive layouts.

The numerical results are shown in Fig. 7~9. It can be seen from Fig. 7 that the applied overlap distance insignificantly affects the overall hydraulic efficiency whether the device is adaptive or non-adaptive. An example of energy flow for case of $y/\overline{w}$= 0.125 is shown in Fig. 8 for both adaptive and non-adaptive devices. A similar trend of energy flow is found for devices with other overlap distances, i.e., $y/\overline{w}$=0.0625, 0.1875, 0.25 resulting in the overall hydraulic efficiency of about 35~39%.

However, the overlap distance has strong influence on the partial hydraulic efficiencies as shown in Fig. 9. By increasing the overlap distance, the amount of water collected by lower reservoirs is decreasing while that of the higher reservoirs is increasing. The overlap ramp reduces the gap between two consecutive ramps, as if the slot width is getting smaller and therefore the water can run-up smoothly. The increase in energy captured by lower reservoirs compensates for the decrease of the higher ones giving insignificant change in overall efficiency. This affects the strategy of power extraction process via multi-stage turbines. The water capture mechanism of both run-up and fall-down processes are shown in Fig. 10~11.

3.2 Multi-stage OWEC installed on breakwater

The investigation concerns the influence of submerged ramp on the performance of land-based OWEC. Table 4 summarizes the specification of submerged ramp.

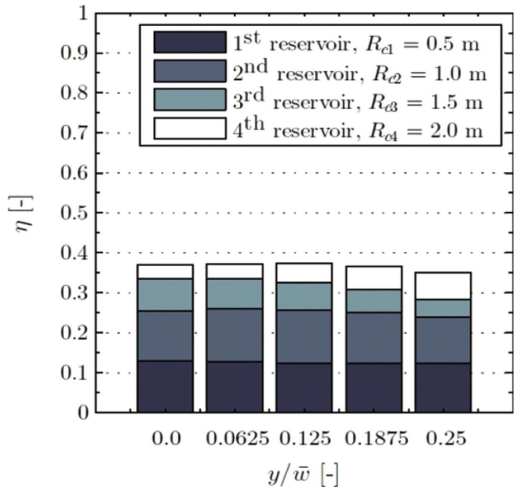

(a) Overlap ramp of adaptive device (w_1 is 1.4$\overline{w}$)

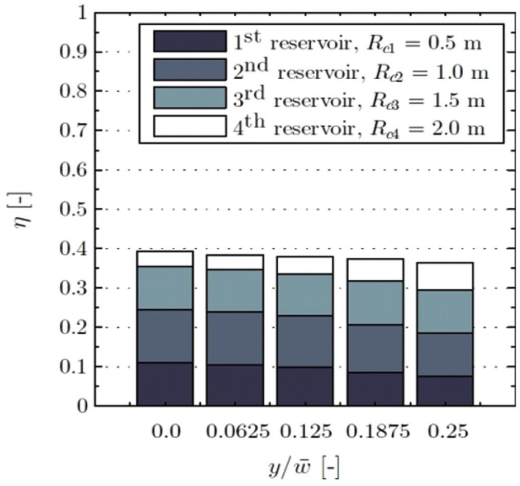

(b) Overlap ramp of non-adaptive device (w_1 is 1.0$\overline{w}$)

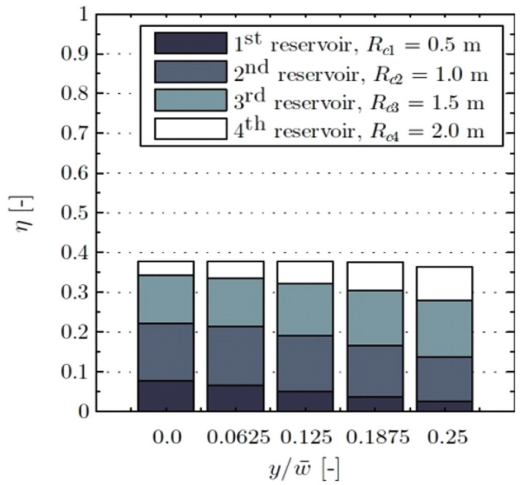

(c) Overlap ramp of adaptive device (w_1 is 0.6$\overline{w}$)

Fig. 9. Partial hydraulic efficiencies of each reservoir versus the relative extended ramp.

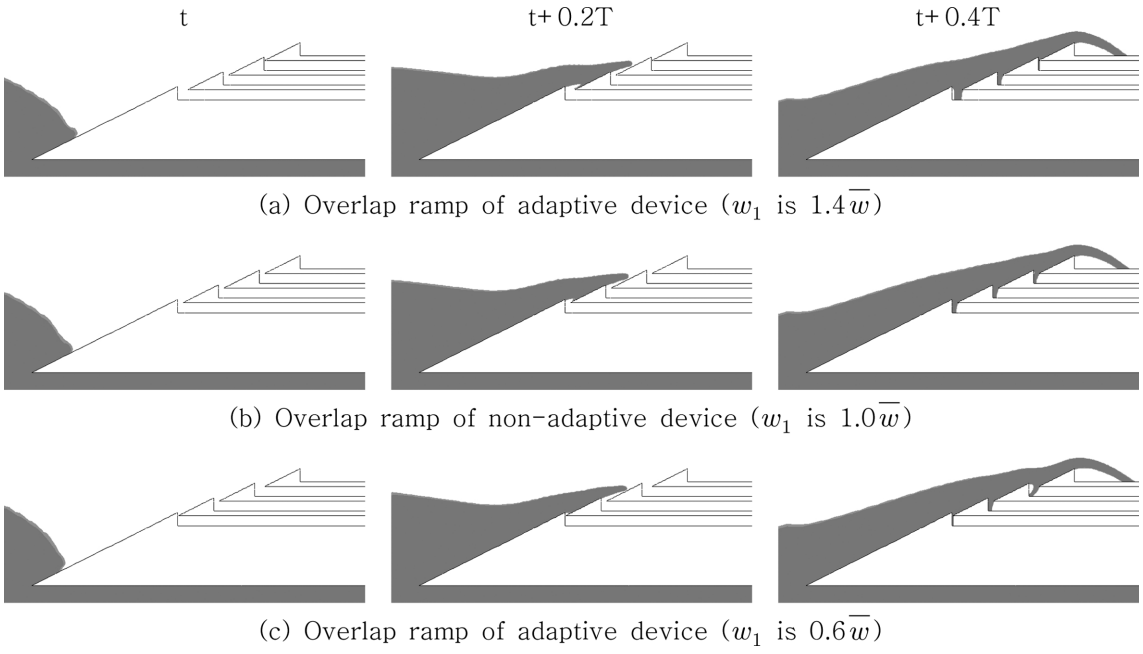

Fig. 10. The water flow run-up processes of overlap ramp multi-stage device based on $y/\overline{w}$=0.25 at different time.

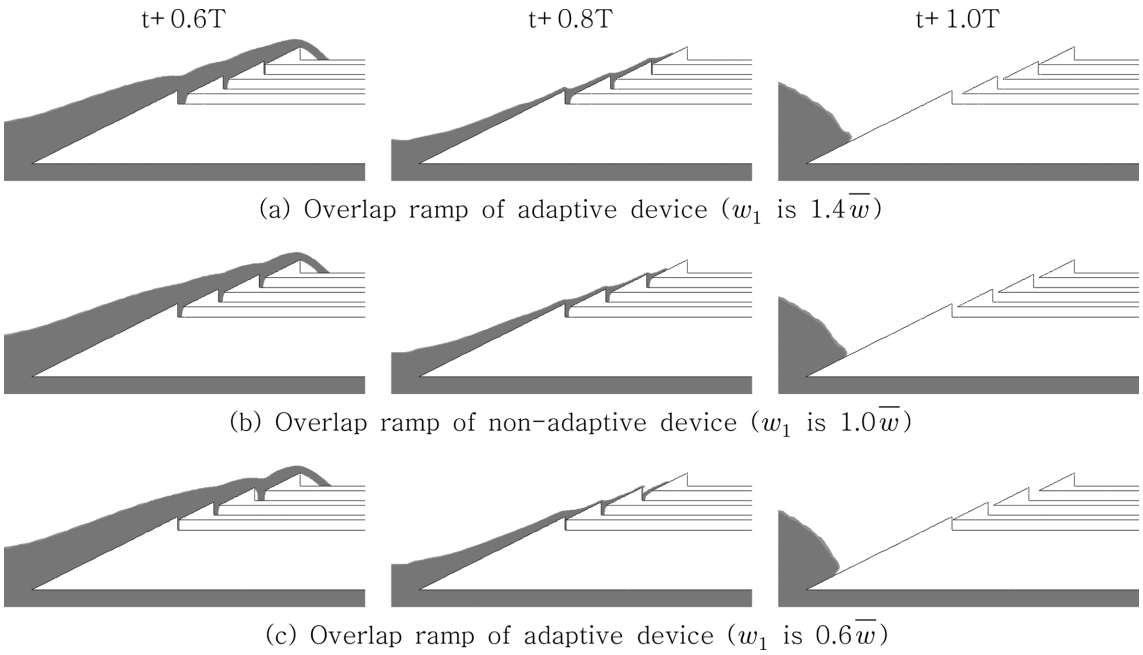

Fig. 11. The water flow fall-down processes of overlap ramp multi-stage device based on $y/\overline{w}$=0.25 at different time.

Table 4. Parameters condition studying effect of submerged ramp

Relative freeboard, R_{c4}/H [-]	1.0
Relative slot width, $\overline{w}/R_{c4}$ [-]	0.2
Submerged depth, R_s [m]	2, 4, 6, 8
Relative submerged depth, R_s/H [-]	1, 2, 3, 4

The overall performance of land-based device is considerably superior compared to that of stationary devices with equivalent submerged ramp as shown in Fig. 12. For small depth, extending the submerged part of ramp results in relatively great performance enhancement. Further extending the ramp gives gradual increase in efficiency and tends to converge to a certain value. Fig. 13a and 13b show partial efficiencies of different submerged depth. The overall performance enhancement is achieved by increasing the energy captured by the highest reservoir, while the lower ones are unaffected.

In case of stationary buoyant devices, a portion of un-cap-

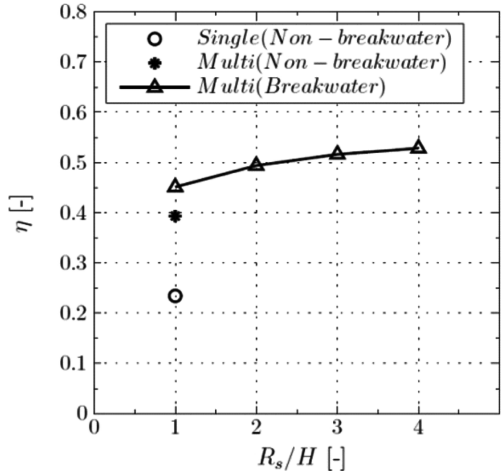

Fig. 12. Overall hydraulic efficiencies of single- and multi-stage device as function of relative submerged depth.

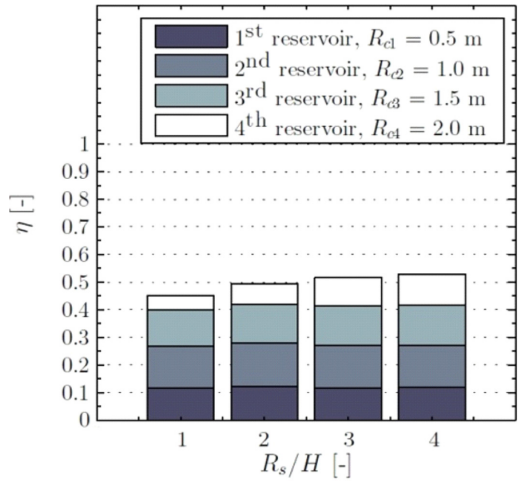

(a) Partial hydraulic efficiencies of each reservoir of multi-stage devices are installed on breakwater as function of relative submerged depth

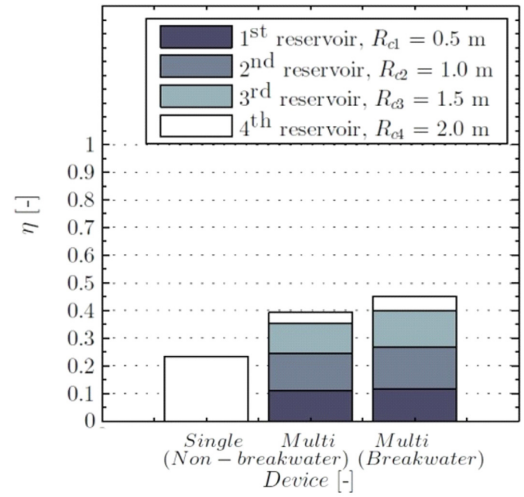

(b) Partial hydraulic efficiencies of each reservoir of single- and multi-stage devices based on relative submerged depth of 1.0

Fig. 13. Effect of submerged depth on overall hydraulic efficiencies of OWEC devices.

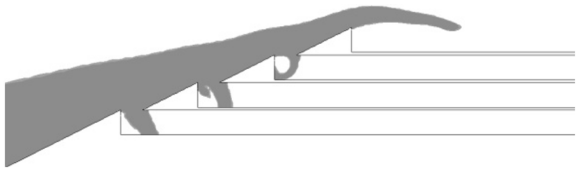

(a) Multi-stage device without breakwater

(b) Multi-stage device installed on breakwater ($R_s/H=1$)

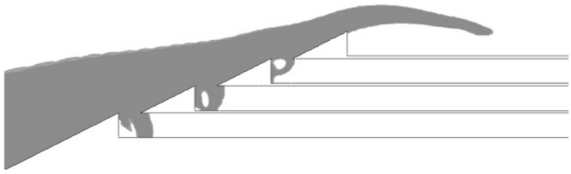

(c) Multi-stage device installed on breakwater ($R_s/H=2$)

Fig. 14. Water flow into reservoirs of multi-stage device with and without breakwater.

tured energy transports with transmission wave. However, a portion of this wave and its energy transforms and runs-up, then overtop into reservoirs in case of land-based devices, resulting in greater efficiency as seen in Fig 14a~14b. Increasing the submerged depth is similar to the effect of wave behavior in shoaling water. Wave shoaling is the effect by which surface waves entering shallower water, resulting in change in wave height, and therefore the amount of water in the higher reservoirs is increasing.

4. Conclusions

Different layouts of multi-stage OWEC devices are numerically investigated in order to study their influence on the performance. The different overlap ramp combined with non-adaptive and adaptive slot width are studied. The numerical results show that the overlap ramp layout slightly effects the overall hydraulic efficiency of OWEC device. However, increasing the overlap distance gives enhancement of hydraulic efficiency of the main reservoir, while that of the lower ones is decreasing. This could affect the strategy of power take-off unit, i.e., turbine.

The OWEC device installed on breakwater gives significant performance enhancement compared to stationary buoyant device. This is because the breakwater eliminates transmission wave and converts part of it into overtopping flow. As the draft is deepened, the efficiency increases and finally tends to converge to a certain value.

Acknowledgements

This research was supported by a grant from National R&D Project “ Development of Wave Energy Converters Applicable to Breakwater and Connected to Micro-Grid with Energy Storage System” funded by Ministry of Oceans and Fisheries, Korea (PMS3600).

References

[1] Brito, A. and Villate, J.L., 2014, Annual Report: Implementing Agreement on Ocean Energy Systems, The Executive Committee of Ocean Energy Systems.

[2] Clément, A. et al., 2002, “Wave energy in Europe: current status and perspectives”, J. Renewable and Sustainable Energy Reviews, Vol. 6, No.5, 405-431.

[3] Connell, K.O. and Cashman, A., 2016, “Development of a numerical wave tank with reduced discretization error”, International Conference on Electrical, Electronics, and Optimization Techniques (ICEEOT).

[4] Du, Q. and Leung, D.Y., 2011, “2D numerical simulation of ocean waves”, in: World Renewable Energy Congress-Sweden; 8-13 May; Linköping; Sweden, Linköping University Electronic Press, No. 057, 2183-2189.

[5] Hu, X.Z. and Liu, S.J., 2014, “Two-dimensional numerical wave tank simulation for deployment of seafloor mining system”, Marine Georesources and Geotechnology Vol. 32, No. 4, 293-306.

[6] Isaacson, M., 1991, “Measurement of regular wave reflection”, J. of Waterway, Port, Coastal and Ocean Eng., Vol. 117, No. 6, 553-569.

[7] Jungrungruengtaworn, S. and Hyun, B.S., 2017, “Influence of slot width on the performance of multi-stage overtopping wave energy converters”, Int. J. Naval Architecture and Ocean Eng., https://doi.org/10.1016/j.ijnaoe.2017.02.005.

[8] Kofoed, J.P., 2002, “Wave Overtopping of Marine Structures: utilization of wave energy”, Ph.D. thesis, Videnbasen for Aalborg UniversitetVBN, Aalborg UniversitetAalborg University, Det Teknisk-Naturvidenskabelige FakultetThe Faculty of Engineering and Science, Institut for Vand, Jord og MiljøteknikDepartment of Civil Engineering.

[9] Kofoed, J.P., 2005, Model testing of the wave energy converter seawave slot-cone generator.

[10] Kofoed, J.P., 2006, “Vertical distribution of wave overtopping for design of multi level overtopping based wave energy converters”, Coastal engineering conference, ASCE American Society of Civil Engineering, Vol. 30, No. 5, 4714.

[11] Liu, Z., Hyun, B.S. and Jin, J.Y., 2008, “Numerical prediction for overtopping performance of OWEC”, J. of Korean Soc. Mar. Environ. Eng., Vol. 11, 35-41.

[12] Liu, Z., Hyun, B.S. and Jin, J.Y., 2009a, “2D Computational analysis of overtopping wave energy convertor”, J. of Korean Soc. of Ocean Engineers, Vol. 23, No.6, 1-6.

[13] Liu, Z., Hyun, B.S. and Jin, J.Y., 2009b, “Computational analysis of parabolic overtopping wave energy convertor”, J. of Korean Soc. Mar. Environ. Eng., Vol. 12, No. 4, 273-278.

[14] Margheritini, L., Vicinanza, D. and Frigaard, P., 2009, “SSG wave energy converter: Design, reliability and hydraulic performance of an innovative overtopping device”, J. Renew. Energ., Vol. 34, 1371-1380.

[15] Minami, M. and Tanaka, H., 2015, “3-D Numerical analysis of overtopping-type wave power generation equipment”, The 25th International Offshore and Polar Engineering Conference, Int. Soc. of Offshore and Polar Eng., Vol. 1, Jul 27.

[16] Nam, B.W. et al., 2008, “Numerical simulation of wave flow over the spiral-reef overtopping device”, The 8th ISOPE Pacific/Asia Offshore Mechanics Symposium, International Society of Offshore and Polar Engineers, Jan 1.

[17] Tanaka, H., Inami, T. and Sakurada, T., 2015, “Characteristics of volume of overtopping and water supply quantity for developing wave overtopping type wave power generation equipment”, The 25th International Ocean and Polar Engineering Conference, International Society of Offshore and Polar Engineerings, Vol. 1, Jul 27.

[18] Thorpe, T.W., 1999, “A brief review of wave energy”, Harwell Laboratory, Energy Technology Support Unit London, AEA Technology, UK.

[19] Van der Meer, J.W. and Janssen, P.F.M., 1995, Wave run-up and wave overtopping at dikes. ASCE book on wave forces on inclined and vertical wall structures, Editor: Z.

[20] Vicinanza, D. and Frigaard, P., 2008, “Wave pressure acting on a seawave slot-cone generator”, J. Coastal Eng., Vol. 55, 553-568.

[21] Victor, L., Troch, P. and Kofoed, J.P., 2011, “On the effects of geometry control on the performance of overtopping wave energy converters”, J. Energies, Vol. 4, No. 10, 1574-1600.

Received 8 March 2017
1st Revised 2 May 2017, 2nd Revised 29 May 2017
Accepted 30 May 2017